OXFORD

Briefings in Bioinformatics, 2022, **23**, 1–11
https://doi.org/10.1093/bib/bbab511
Problem Solving Protocol

Predicting drug–drug interactions by graph convolutional network with multi-kernel

Fei Wang, Xiujuan Lei, Bo Liao and Fang-Xiang Wu

Corresponding author: Fang-Xiang Wu, 3B42, 57 Campus Drive, Saskatoon, S7N 5A9, Canada. Tel: ++(306)966-5280; Fax: +1(306)966-5280; E-mail: fangxiang.wu@usask.ca

Abstract

Drug repositioning is proposed to find novel usages for existing drugs. Among many types of drug repositioning approaches, predicting drug–drug interactions (DDIs) helps explore the pharmacological functions of drugs and achieves potential drugs for novel treatments. A number of models have been applied to predict DDIs. The DDI network, which is constructed from the known DDIs, is a common part in many of the existing methods. However, the functions of DDIs are different, and thus integrating them in a single DDI graph may overlook some useful information. We propose a graph convolutional network with multi-kernel (GCNMK) to predict potential DDIs. GCNMK adopts two DDI graph kernels for the graph convolutional layers, namely, increased DDI graph consisting of 'increase'-related DDIs and decreased DDI graph consisting of 'decrease'-related DDIs. The learned drug features are fed into a block with three fully connected layers for the DDI prediction. We compare various types of drug features, whereas the target feature of drugs outperforms all other types of features and their concatenated features. In comparison with three different DDI prediction methods, our proposed GCNMK achieves the best performance in terms of area under receiver operating characteristic curve and area under precision-recall curve. In case studies, we identify the top 20 potential DDIs from all unknown DDIs, and the top 10 potential DDIs from the unknown DDIs among breast, colorectal and lung neoplasms-related drugs. Most of them have evidence to support the existence of their interactions. fangxiang.wu@usask.ca

Keywords: graph convolutional network, drug–drug interaction, drug features, drug repositioning

Introduction

Drug repositioning is to find novel usages for existing drugs. The safety and other properties of the existing drugs, which have been approved to sell on the market, have been studied clearly. Therefore, drug repositioning helps save time and reduce costs of drug development greatly. Several successful drugs have been proposed by drug repositioning approaches, such as sildenafil, thalidomide, zidovudine, minoxidil and celecoxib [1].

In order to increase the prediction efficiency, many computational approaches have been utilized to predict potential drugs for different diseases. A main field is predicting potential links between drugs and related elements, such as drug–disease associations (DDAs) [2–7], drug–target interactions [8–13] and drug–drug interactions (DDIs) [14–21]. When predicting DDAs, Luo *et al.* calculated similarities and constructed a similarity network [2, 3]. Random walk was employed to calculate the probabilities of DDAs. Li *et al.* utilized a convolutional neural network (CNN) model to conduct a binary classification of DDAs, based on the known DDAs and drug/disease feature vectors [5]. In the study of DTI, deep learning (DL) approaches are effective tools to predict potential DTIs. Wen *et al.* constructed a deep-belief network to predict potential DTIs [9]. Monteiro *et al.* combined a CNN with a deep neural network (DNN) to make predictions, where the CNN was used to produce novel representations of feature vectors and the DNN was employed to predict DTIs [12].

The DDIs refer to the pharmacological and clinical responses to a drug combination, different from the known effects of two drugs when used alone. The prediction of DDIs helps researchers to have a deep understanding of the mechanisms of actions of drugs. In order to analyze DDIs, various types of drug features have been studied, such as chemical substructures, side effects, targets, pathways and enzymes, etc.

A number of approaches have been proposed to predict DDIs based on one or more types of drug features. Ferdousi *et al.* calculated drug–drug similarities based

Fei Wang is current a PhD candidate in the Division of Biomedical Engineering at the University of Saskatchewan. His research topic is bioinformatics, machine/deep learning and drug repositioning.
Xiujuan Lei has been a professor in Shaanxi Normal University since 2013. Her research interests include bioinformatics, data mining, swarm intelligence computing and machine/deep learning.
Bo Liao is currently working in Hainan Normal University as a professor. His current research interests include bioinformatics, data mining and machine/deep learning.
Fang-Xiang Wu is currently a full professor in three Departments (Computer Science, Biomedical Engineering and Mechanical Engineering) at the University of Saskatchewan. His research interests include artificial intelligence, machine/deep learning, computational biology and bioinformatics, medical image analytics, complex network analytics. He is an IEEE senior member.
Received: September 14, 2021. **Revised:** October 28, 2021. **Accepted:** November 7, 2021

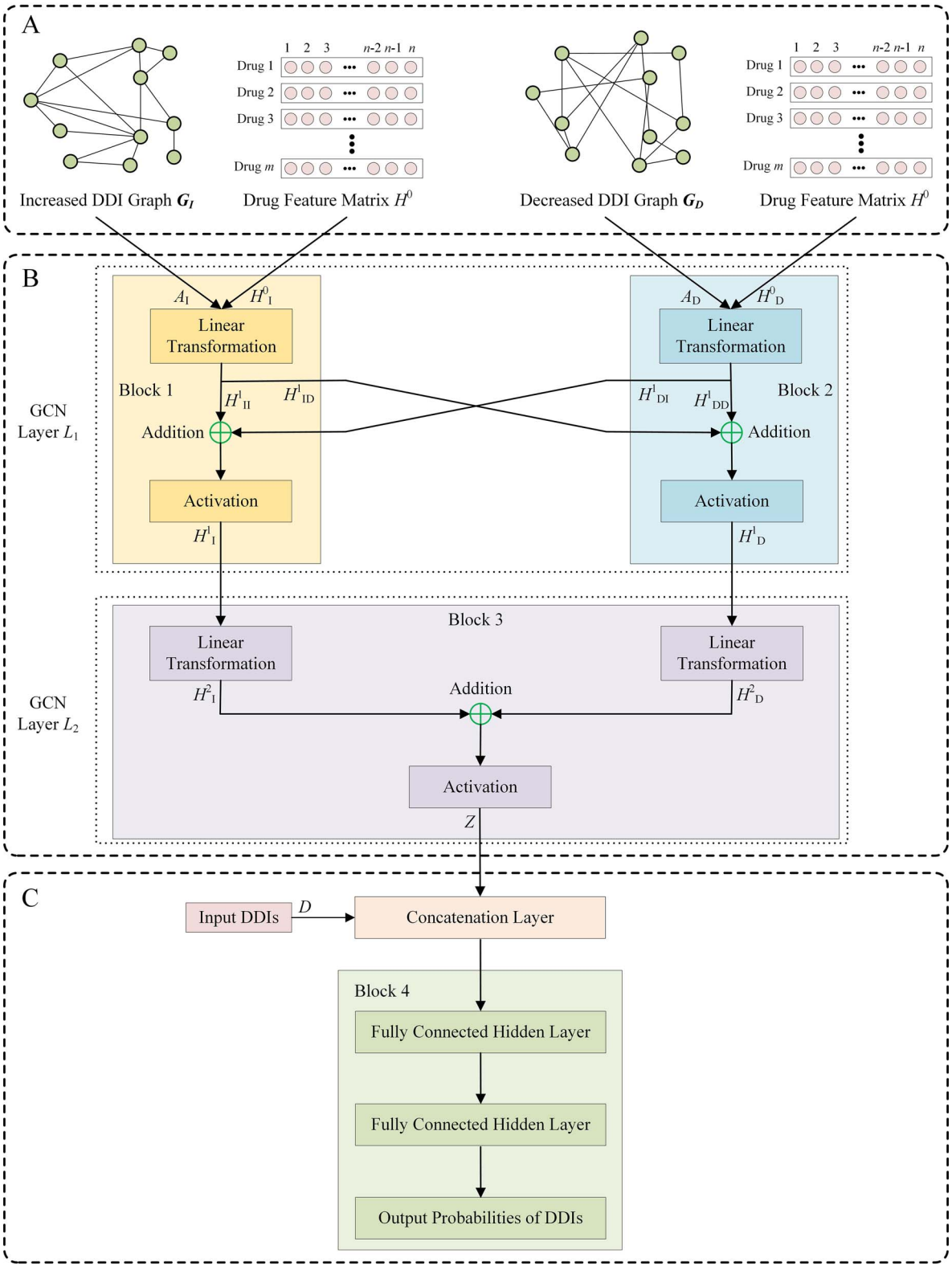

Figure 1. The architecture of GCNMK. **A**: Constructing two DDI graphs from increased, decreased interactions, and inputting drug attributes. **B**: Generating the feature representation of drugs by GCN. **C**: Predicting DDIs.

on various types of features and utilized a positive similarity threshold to determine the potential DDIs [14]. However, the similarities of many DDIs are negative, while they cannot be predicted by a constant positive value. Yan *et al.* used a *k*-nearest neighbor procedure after generating similarities of known DDIs and employed a regularized least squares classifier to predict potential DDIs [15]. In the classifier, both positive samples and negative samples are essential. In predicting potential DDIs, the positive samples are those known DDIs, whereas the

negative samples are the unknown DDIs. Zheng *et al.* used an SVM model to produce reliable negative samples from the unknown samples and made a further prediction [16]. Zhang *et al.* proposed a multi-modal autoencoder (MDAE) with positive-unlabeled learning to predict potential DDIs [21].

The DDIs can be utilized to construct a DDI graph, where nodes are drugs and edges are interactions among drugs. Zhou *et al.* used a Markov clustering algorithm on the DDI graph to predict potential drug combinations [17]. Additionally, researchers can combine the drug features with the network structures to predict potential interactions. Zhang *et al.* used a random walk algorithm on the DDI graph [18], while the transition probabilities were based on the drug–drug similarity matrices.

Graph convolutional network (GCN) [22] is a variant of CNN on the graph, while the graph is used as a kernel. Researchers utilize GCN to produce low-dimensional representation vectors of drugs by learning topological structures of drugs in the DDI graph. Feng *et al.* combined GCN with a deep neural network to generate feature representation matrix and predict potential DDIs [19]. Huang *et al.* added a skip graph to reflect the indirect connections in the original DDI graph and made predictions based on both the original DDI graph and the skip graph [20].

In many DDI prediction methods, researchers do not distinguish the responses of DDIs. All known DDIs are labeled as positive samples and used to construct the DDI graph. However, there are many types of DDIs relating to various mechanisms. About half of them are 'increase'-related, such as 'DRUG A may increase the activities of DRUG B', another half of them are 'decrease'-related, such as 'The metabolism of DRUG A can be decreased when combined with DRUG B'.

In this work, we aim to learn novel embeddings from those two types of DDIs. As discussed above, GCN is an effective structure to utilize both DDI graphs and drug feature vectors. We propose a graph convolutional network with multi-kernel (GCNMK) to predict potential increased DDIs. We firstly construct an increased DDI graph and a decreased DDI graph from the increase'-related and 'decrease'-related DDIs, respectively. Two GCN layers are combined to learn low-dimensional representation vectors of drugs with those two graphs and various types of drug features. After generating the node embeddings, two drug vectors are concatenated to be the vector of a DDI. Finally, a block with three fully connected layers is used to make predictions. In the experiments, we investigate the prediction performance of our proposed model on various types of drug features, including chemical substructures, side effects, targets, pathways and enzymes, etc. We compare three state-of-the-art methods with our GCNMK. The results demonstrate that our GCNMK outperforms other competing methods in predicting potential DDIs. In case studies, we predict potential DDIs, and most of them have evidence to support the existence of their interactions.

Methods

In this section, we introduce the architecture of our GCNMK model, as shown in Figure 1. In Figure 1**A**, an increased DDI graph and a decreased DDI graph are constructed from the 'increase'-related and 'decrease'-related DDIs, respectively. The two graphs and drug feature matrices are fed into two GCN blocks, respectively. In Figure 1**B**, these two GCN blocks form the GCN layer L_1, whereas layer L_2 contains the third block. An addition procedure, whose output is a linear combination of its inputs, is adopted in each block to generate drug embeddings from both increased and decreased DDI graphs. The low-dimensional representation vectors of drugs are produced after the layer L_2. In Figure 1**C**, the feature vectors of two drugs are concatenated to form a DDI vector. A block with three fully connected layers is employed to predict potential DDIs.

DDI graphs and drug feature matrix

A DDI graph $G = (V, E)$ represents a collection of n nodes and m edges, while nodes are drugs and edges are DDIs, which is described by an association matrix A. The DDI refers to the pharmacological and clinical responses to a drug combination, different from the known effects of two drugs when used alone. If there is a known response between drugs i and j, in the association matrix A, $A(i, j) = 1$. Otherwise, $A(i, j) = 0$. The DDI graph is undirected, that is, $A(i, j) = A(j, i)$.

There are various types of responses between two drugs, including analgesic activity, risk or severity of heart failure, serum concentration, therapeutic efficacy, etc. We divide them into two groups. One group contains DDIs that increase one of the responses, whereas another group contains DDIs that decrease one of the responses. Two DDI graphs G_I and G_D are constructed based on those two groups of DDIs, respectively. Their association matrices are denoted by A_I and A_D.

Another matrix is the drug feature matrix H^0. In order to make a distinction, the feature matrix together with the graph G_I is marked as H_I^i, whereas the other one is H_D^i, at the i-th layer of GCNs.

Feature representations of drugs

In this study, we construct two DDI graphs G_I and G_D for the increased and decreased DDIs, respectively. Our purpose is to use GCN layers to learn features from both two graphs. In layer L_1, two blocks are adopted, each has an input graph, as shown in Figure 1**B**. The propagation rules of linear transformation are as follows:

$$H_{II}^1 = F_I H_I^0 W_I^0 \tag{1}$$

$$H_{ID}^1 = F_I H_I^0 W'^0_I \tag{2}$$

$$H_{DD}^1 = F_D H_D^0 W_D^0 \tag{3}$$

$$H_{DI}^1 = F_D H_D^0 W'^0_D \tag{4}$$

where H_{II}^1 and H_{DD}^1 are the node embedding matrices transferring within each block, respectively. H_{ID}^1 and H_{DI}^1 transferring between the two blocks in layer L_1. $F_I = \widetilde{D}_I^{-\frac{1}{2}}\widetilde{A}_I\widetilde{D}_I^{-\frac{1}{2}}, F_D = \widetilde{D}_D^{-\frac{1}{2}}\widetilde{A}_D\widetilde{D}_D^{-\frac{1}{2}}$. $\widetilde{A}_I = A_I + I$ and $\widetilde{A}_D = A_D + I$ are the association matrices of the graph G_I and G_D, respectively. I is the identity matrix. $\widetilde{D}_I(i,i) = \sum_j \widetilde{A}_I(i,j)$ and $\widetilde{D}_D(i,i) = \sum_j \widetilde{A}_D(i,j)$ are the degree diagonal matrices.W_I^0, W'^0_I, W_D^0 and W'^0_D are the weight matrices.

In each block, an addition procedure is adopted before the activation function as follows:

$$H_I^1 = \sigma(H_{II}^1 + H_{DI}^1) \tag{5}$$

$$H_D^1 = \sigma(H_{DD}^1 + H_{ID}^1) \tag{6}$$

where H_I^1 and H_D^1 are the outputs. σ is the activation function, which is ReLU in this study.

The GCN layer L_2 contains Block 3, which is used to integrate the outputs from two blocks in layer L_1 as follows:

$$Z = \sigma(H_I^2 + H_D^2) = \sigma(F_I H_I^1 W_I^1 + F_D H_D^1 W_D^1) \tag{7}$$

where Z is the final representation matrix of drugs.

Predicting DDIs

The Block 4 with three fully connected layers is utilized to predict DDIs in our model, as shown in Figure 1**C**. Before Block 4, a concatenation layer is used to generate the DDI feature matrix. The inputs of concatenation layer are representation matrix Z, and DDI information matrix D. For a pair of drugs i and j in D, its DDI feature vector is the concatenation of Z_i and Z_j, represented as $[Z_i, Z_j]$, where Z_i and Z_j are the feature vectors of drugs i and j in Z, which is fed into Block 4.

In Block 4, the number of neurons in each layer is 64, 16 and 1. The DDI prediction is formulated as a binary classification that the output values are the probabilities of how likely a drug pair is a true DDI. The activation function is ReLU in hidden layers and Sigmoid in output layer.

The cross-entropy loss function is used in our GCNMK model:

$$BCE = -\frac{1}{N}\sum_{ij}[y_{ij}\log p_{ij} + (1 - y_{ij})\log(1 - p_{ij})] \tag{8}$$

where N is the sample size, $y_{ij} \in [0, 1]$ is the true label for the interaction between drug i and j. '1' represents the label of a positive sample, whereas '0' represents that of a negative sample. p_{ij} is the predicted probability.

In order to prevent the over-fitting problem, an L_2-regularization is adopted:

$$L_2 = \frac{\lambda}{2N}\sum_w w^2 \tag{9}$$

where λ is a hyper-parameter, w is an element in the parameter matrices W_I^0, W'^0_I, W_D^0, W'^0_D, W_I^1 and W_D^1. As a result, the loss function for training our GCNMK model is $L = BCE + L_2$.

Experiments

In this section, we illustrate the performances of our proposed model in various types of data and compare it with three state-of-the-art DDI prediction algorithms. Five aspects are discussed in the following five subsections: datasets in both our proposed model and the competing models; experiment setting; visualization analysis of embedding features; results of competing methods; case studies of our proposed model.

Datasets

In order to make a fair comparison between various types of features and methods, we choose the drugs that have all types of features in both our proposed methods and the competing methods. In our study, we download DDIs from the DrugBank database (Version 5.1.8) [23], whereas the numbers of 'increase'-related and 'decrease'-related DDIs are 40 202 and 40 500, respectively, among 613 FDA-approved drugs.

Eight types of features are compared in the experiments, as described in Table 1. It should be mentioned that the node2vec feature matrix is generated from the whole DDI graph $G_{all} = G_I \cup G_D$ and that there is an information leak in it. The features about associated drugs, enzymes, side effects, substructures and targets are generated from the corresponding databases, as listed in Table 1. The pathway feature vectors of drugs are based on the drug-related targets and target–pathway associations. The prototype ranked list (PRL) feature vector is generated by merging a group of profiles of a given drug into a single ranked list [29]. The profiles are downloaded from the Library of Integrated Network-based Cellular Signatures (LINCS) database [28].

Experiment setting

In this study, we use 5-fold cross-validation (5-CV) to evaluate the prediction performance of our GCNMK model and the competing methods. The known DDIs are represented as positive samples, and the unknown DDIs are represented as negative samples. The number of positive samples is 80 702, whereas that of negative samples is 106 876. In order to make the training data balanced, 80 702 negative samples are randomly selected. Both the positive samples and the selected negative samples are divided into five subsets randomly. At each time, a positive subset and a negative subset

Table 1. The types of features, their dimensions, and resources/methods

Feature types	Dimensions	Resources
Associated Drugs	613	DrugBank ([23])
Enzymes	454	DrugBank
Pathways	533	DrugBank, CTD ([24]) and KEGG ([25])
Side Effects	4859	SIDER ([26])
Substructures	811	DrugBank
Targets	2670	DrugBank and CTD
Node2vec	613	DrugBank, [27] and [20]
PRL	978	LINCS ([28] and [29])

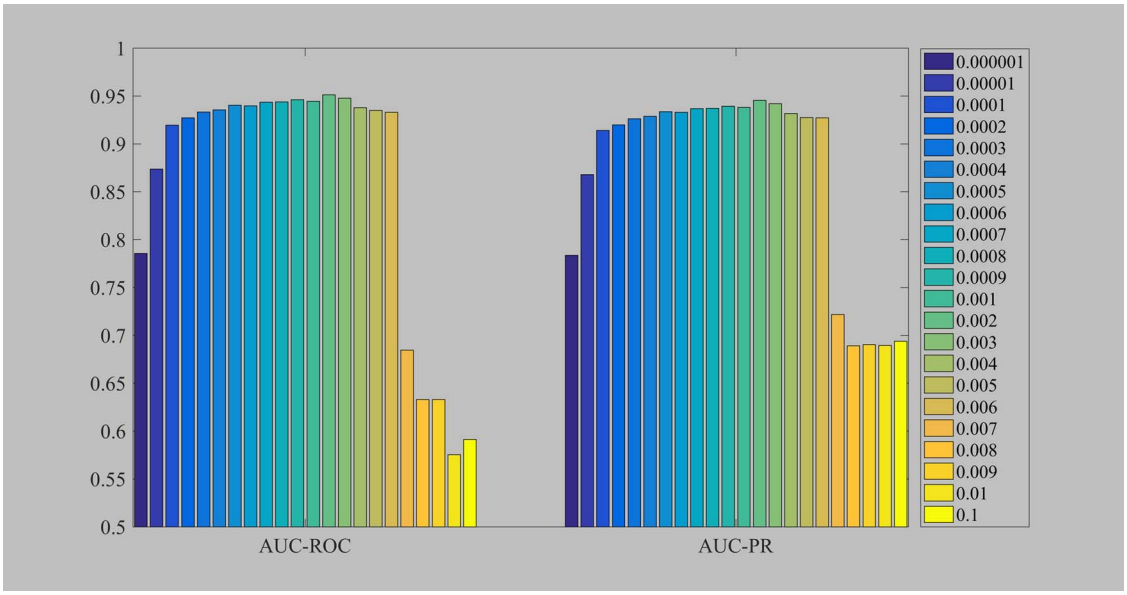

Figure 2. The influence of learning rate *lr*.

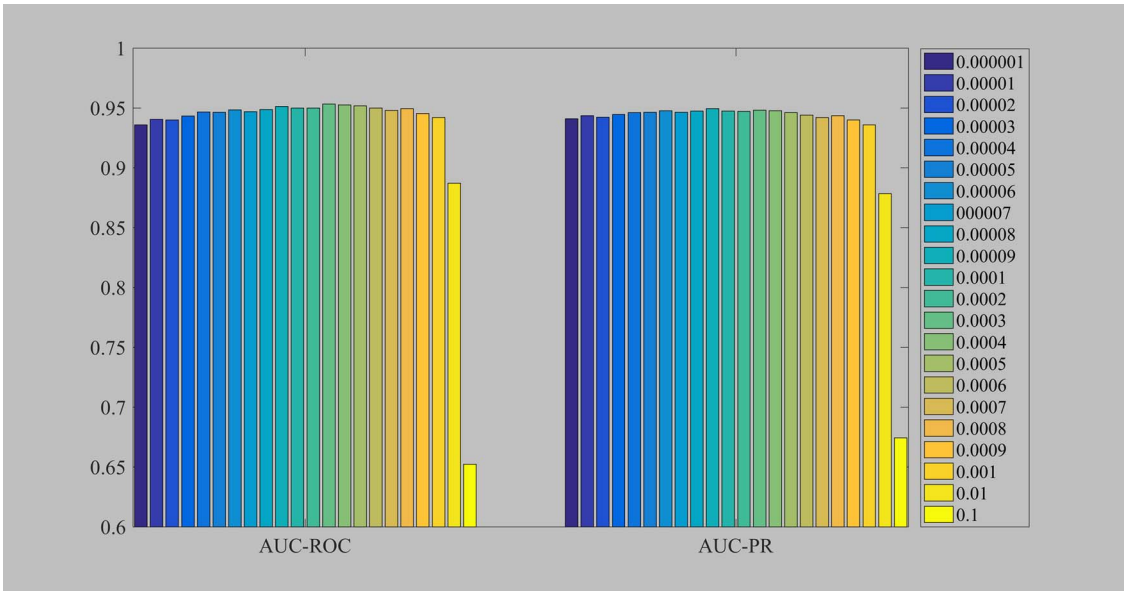

Figure 3. The influence of L_2-regularization coefficient λ.

are selected as the testing set, whereas the remaining subsets are selected as the training set. After five times, all subsets are used up to be testing sets, and the predicting results are produced.

In order to avoid using the testing information in the training procedure and make the testing procedure more accurate, the DDIs in the testing set are deleted from G_I and G_D at each training.

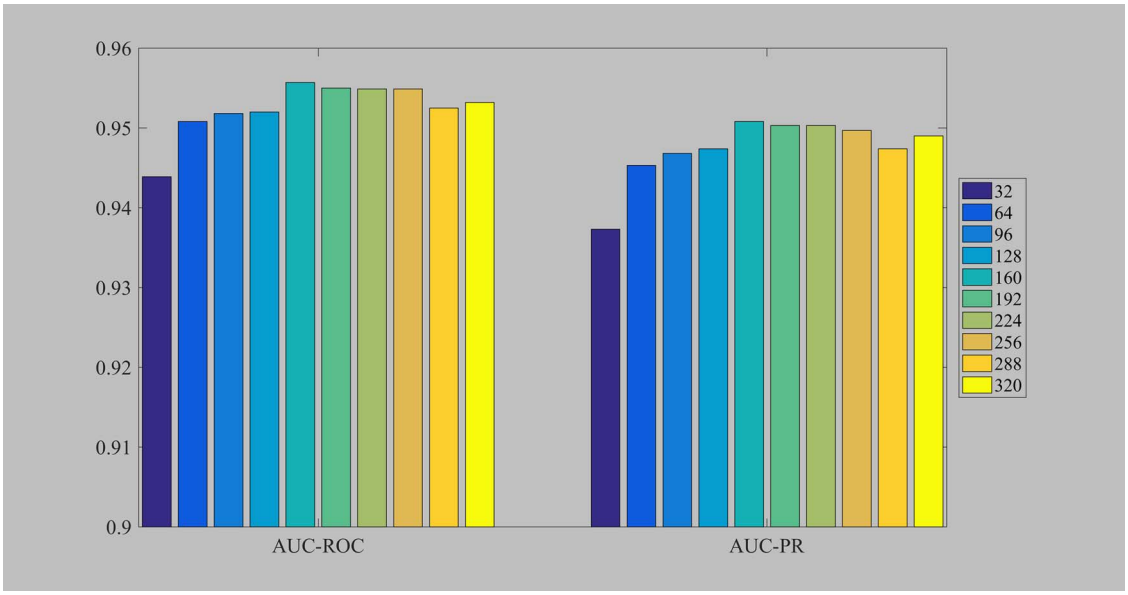

Figure 4. The influence of embedding size d.

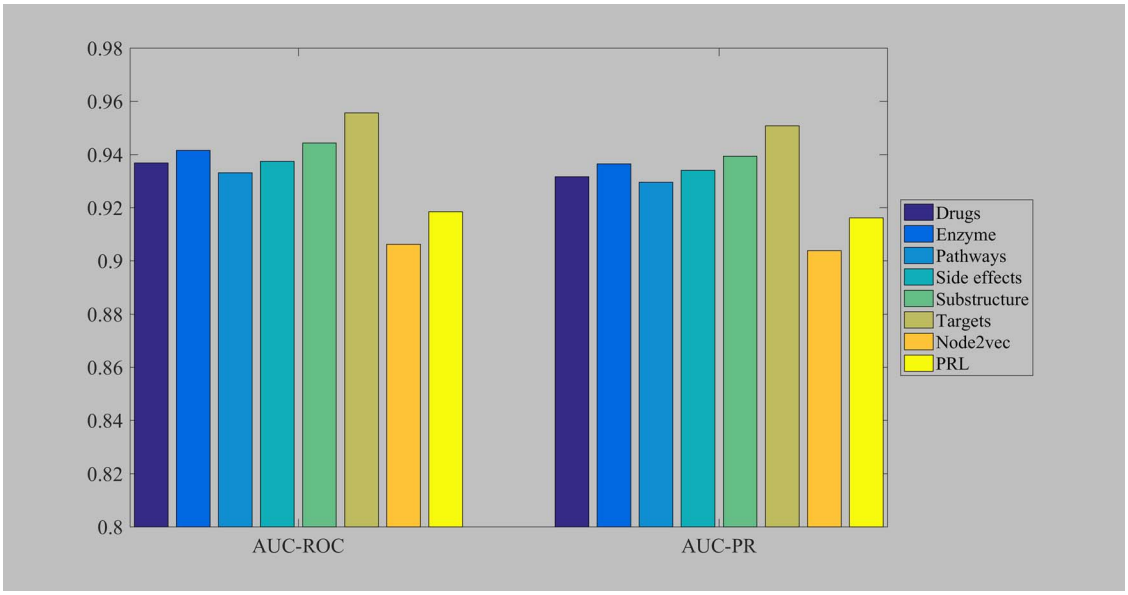

Figure 5. The influence of feature type.

In experiments, the area under receiver operating characteristic curve (AUC-ROC) and area under precision-recall curve (AUC-PR) are used to measure the performance of results. The higher the values are, the more reliable the model is.

We adjust the parameters in order to achieve optimal performances. For the learning rate lr, L_2-regularization coefficient λ, and embedding size d, we search for the optimal values with the nominal values lr=0.0005, λ=0.0005, d=128. When optimizing the influence of a specific parameter, the other two parameters are set to be the nominal values. After optimization, its optimal value is used to update its nominal value. In those experiments, the target information is used to construct the drug feature matrix H^0.

The learning rate $lr \in [0.1, 0.01, 0.001, 0.0001, 0.00001, 0.000001]$. After achieving that the optimal value is around 0.001, we set the learning rate to be in a refined range [0.0001,0.0002,...,0.0009,0.001,0.002,...,0.009]. In order to show them clearly, we use two histograms to depict the AUC-ROC and AUC-PR values under different lr values, as shown in Figure 2. When lr increases from 0.000001 to 0.002, the general trend of AUC-ROC and AUC-PR is ascending. When lr is larger than 0.002, the AUC-ROC and AUC-PR are reducing. Therefore, we set the learning rate lr to be 0.002 in our proposed GCNMK model.

The L_2-regularization coefficient $\lambda \in [0.1, 0.01, 0.001, 0.0001, 0.00001, 0.000001]$. The optimal value is around 0.0001. Then λ is set to be in a refined range [0.00001,

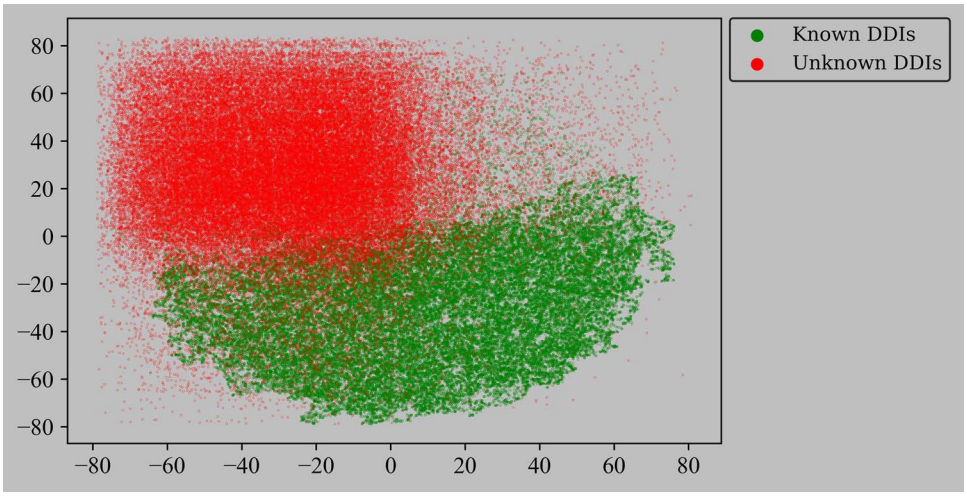

Figure 6. The t-SNE visualization analysis of embeddings.

Table 2. The prediction performances of the competing methods

Methods	AUC-ROC			AUC-PR		
	Ave.	Std.	Rank	Ave.	Std.	Rank
GCNMK	**0.9557**	0.0017	1	**0.9508**	0.0012	1
GCNMK-5	0.9337	0.0042	2	0.9292	0.0048	2
DPDDI	0.9126	0.0003	3	0.9131	0.0003	4
SkipGNN	0.8589	0.0005	5	0.8604	0.0005	5
MDAE	0.8981	0.0015	4	0.9232	0.0013	3

Ave.: The average value across ten repeats. Std.: The standard deviation across ten repeats. Rank: The ranks are based on the average values.

0.00002,...,0.00009, 0.0001, 0.0002,...,0.0009]. All the AUC-ROC and AUC-PR values are shown in Figure 3. When λ increases from 0.000001 to 0.0003, the AUC-ROC and AUC-PR increase slightly. When λ is larger than 0.0003, the AUC-ROC and AUC-PR are decreasing. Therefore, we set λ to be 0.0003 in our proposed GCNMK model.

The embedding size $d \in [32, 64, 96, 128, 160, 192, 224, 256, 288, 320]$. The prediction performance changes a little when the embedding size varies, as depicted in Figure 4. When d is increasing from 32 to 160, the AUC-ROC and AUC-PR are increasing. When d is larger than 160, the AUC-ROC and AUC-PR are becoming smaller. We set the optimal embedding size d to be 160 in our GCNMK model.

Various types of features are used in our GCNMK model. The histograms of their prediction performance are shown in Figure 5. Although the node2vec [27] feature has a problem of information leak, its prediction performance is the worst among the eight types of features. The PRL [29] feature produces the 2nd-worst prediction results. The differences of the AUC-ROC and AUC-PR of the other six types of features are not large, and the target feature of drugs achieves the best prediction performance among them. Therefore, in the following comparison, we use the target feature of drugs in our GCNMK model.

We compare our methods with three DDI prediction methods, which are DPDDI [19], SkipGNN [20] and MDAE [21]. The parameters are set to be the optimal values as described in their methods. The type of feature used in DPDDI is the associated drugs. In SkipGNN, it is node2vec. Five types of features are used in MDAE, including associated drugs, enzymes, pathways, targets and substructures. Additionally, the same five types of features are used in our GCNMK model, which is represented as GCNMK-5 in Table 2.

Visualization analysis of embedding features

In order to study the embedding performance of our proposed model, we employ t-distributed stochastic neighbor embedding (t-SNE) [32] to visualize DDIs based on the embedding features learned from our model. t-SNE is applied to reduce the dimensionality of embedding features to 2 and plot a 2-D figure, as shown in Figure 6. The green dots are known DDIs, whereas the red dots are unknown DDIs. Based on Figure 6, we can see that most of dots are gathered in two areas. Specially, the known DDIs are located at the lower half of the figure, whereas the unknown DDIs are located on the upper right quarter of the figure, which can explain the performance of our model.

Results

The prediction performances of all competing methods are listed in Table 2. Each method is repeated 10 times to generate an average value and an SD of the AUC-ROC and AUC-PR metrics. The GCNMK and GCNMK-5, whose performance ranks are 1 and 2 in terms of AUC-ROC

Table 3. The top 20 predicted DDIs

Rank	Drug A	Drug B	Evidence Source	Description
1	Imipramine	Olanzapine	Drugs.com	Using imipramine together with olanzapine may increase side effects such as drowsiness.
2	Olanzapine	Theophylline	TWOSIDE	Using the drug combination may increase the side effect of anaemia.
3	Desipramine	Olanzapine	Drugs.com	Using desipramine together with olanzapine may increase side effects such as drowsiness.
4	Sulfadiazine	Trimethoprim	TWOSIDE	Using the drug combination may increase the side effect of anaemia.
5	Cimetidine	Tramadol	Drugs.com	Cimetidine may increase the blood levels and effects of tramadol.
6	Sulfamethoxazole	Trimethoprim	TWOSIDE	Using the drug combination may increase the side effect of anaemia folate deficiency.
7	Hydrochloroth-iazide	Metoprolol	Drugs.com	Using metoprolol and hydrochlorothiazide together may lower your blood pressure and slow your heart rate.
8	Ofloxacin	Ticlopidine	N.A.	N.A.
9	Dextromethor-phan	Quinidine	Drugs.com	Using dextromethorphan together with quinidine may increase the effects of dextromethorphan.
10	Tolbutamide	Vincristine	N.A.	N.A.
11	Estradiol	Progesterone	TWOSIDE	Using the drug combination may increase the side effect of anaemia.
12	Fosinopril	Hydrochloroth-iazide	Drugs.com	Their effects may be additive on lowering your blood pressure.
13	Nicotine	Vincristine	TWOSIDE	Using the drug combination may increase the side effect of anaemia.
14	Hydrochloroth-iazide	Pindolol	Drugs.com	Using pindolol and hydrochlorothiazide together may lower your blood pressure and slow your heart rate.
15	Lorazepam	Ranitidine	TWOSIDE	Using the drug combination may increase the side effect of anaemia.
16	Promethazine	Pseudoephedrine	TWOSIDE	Using the drug combination may increase the side effect of anaemia.
17	Theophylline	Vincristine	TWOSIDE	Using the drug combination may increase the side effect of neutropenia.
18	Panobinostat	Rosiglitazone	N.A.	N.A.
19	Hydralazine	Reserpine	N.A.	N.A.
20	Ranitidine	Teniposide	N.A.	N.A.

N.A.: The evidence of the given DDI is not available till now.

and AUC-PR, respectively, are our proposed methods. The ranks of other three competing methods are from 3 to 5.

We compare GCNMK model with others in different aspects. There is only one graph kernel in DPDDI method [19], which is the graph of all known DDIs $G_{all} = G_I \cup G_D$. The AUC-ROC and AUC-RP values produced by GCNMK model are about 4% larger than those of DPDDI. Referring to the results in Figure 5, our GCNMK model still achieves better performance than DPDDI when using the same type of feature. The results indicate that using two DDI graphs G_I and G_D can improve the prediction performance.

There are two graph kernels in SkipGNN [20] that one kernel is G_{all} and another kernel G_{skip} is based on G_{all}. The GCNMK generates 10% larger AUC-ROC and AUC-RP values than SkipGNN. In this way, the graphs G_I and G_D work better in predicting potential DDIs. One possible reason is that the ratio of edges in G_{all} is about 43% in our datasets, and it is nearly 95% in G_{skip}. Adding such an almost fully connected graph can not improve the prediction performance.

Five types of features are used to identify the drug representation feature vectors in GCNMK-5 and MDAE [21]. In the results, the GCNMK-5 outperforms MDAE. Furthermore, the GCNMK achieves better prediction performance than GCNMK-5, which indicates that multiple types of features do not achieve better results than a single type of feature.

In summary, our proposed GCNMK model achieves the best prediction performance among all competing methods in terms of AUC-ROC and AUC-PR.

Case studies

In case studies, all 106 876 unknown DDIs are fed into our GCNMK model. A larger prediction score of two drugs suggests that they have a higher probability of having an interaction. We generate a ranked list of DDIs in descending order according to their prediction scores.

The top 20 predicted DDIs are listed in Table 3. We verify them with TWOSIDE database [30] and Drug Interactions Checker [31], and collect the descriptions

Table 4. The top ten predicted DDIs of breast neoplasms-related drugs

Rank	Drug A	Drug B	Evidence Source	Description
1	**Verapamil**	Mefloquine	Drugs.com	Using mefloquine together with verapamil can increase the risk of irregular heart rhythm that may be serious and potentially life-threatening.
2	**Sulindac**	Methazolamide	N.A.	N.A.
3	**Ranitidine**	**Vinblastine**	TWOSIDE	Using the drug combination may increase the side effect of neutropenia.
4	**Rosiglitazone**	Metformin	TWOSIDE	Using the drug combination may increase the side effect of anaemia vitamin b12 deficiency.
5	**Quinine**	Nizatidine	TWOSIDE	Using the drug combination may increase the side effect of chest pain.
6	**Sulindac**	Theobromine	N.A.	N.A.
7	**Ranitidine**	Sunitinib	TWOSIDE	Using the drug combination may increase the side effect of anaemia.
8	**Ranitidine**	Teniposide	N.A.	N.A.
9	**Ranitidine**	**Vinorelbine**	TWOSIDE	Using the drug combination may increase the side effect of anaemia.
10	**Sulfasalazine**	Isosorbide	TWOSIDE	Using the drug combination may increase the side effect of anaemia.

The breast neoplasms-related drugs are in bold.

Table 5. The top ten predicted DDIs of colorectal neoplasms-related drugs

Rank	Drug A	Drug B	Evidence Source	Description
1	**Simvastatin**	Niacin	TWOSIDE	Using the drug combination may increase the side effect of iron deficiency anaemia.
2	**Fluorouracil**	Lorazepam	TWOSIDE	Using the drug combination may increase the side effect of iron deficiency anaemia.
3	**Meloxicam**	**Methotrexate**	TWOSIDE	Using the drug combination may increase the side effect of iron deficiency anaemia.
4	**Fluorouracil**	Tramadol	TWOSIDE	Using the drug combination may increase the side effect of anaemia.
5	**Famotidine**	Primidone	TWOSIDE	Using the drug combination may increase the side effect of haemorrhagic anaemia.
6	**Dacarbazine**	Phenytoin	N.A.	N.A.
7	**Famotidine**	Progesterone	TWOSIDE	Using the drug combination may increase the side effect of atrial fibrillation.
8	**Fluorouracil**	Oxymetholone	N.A.	N.A.
9	**Doxorubicin**	Lynestrenol	N.A.	N.A.
10	**Simvastatin**	Trifluoperazine	TWOSIDE	Using the drug combination may increase the side effect of pancytopenia.

The colorectal neoplasms-related drugs are in bold.

about their interactions. For instance, the description of 'Imipramine-Olanzapine' is 'Using imipramine together with olanzapine may increase side effects such as drowsiness'. We can see that 15 DDIs are confirmed in either Drugs.com or TWOSIDE. The results indicate that our proposed GCNMK model is effective in predicting novel DDIs. Other five DDIs, 'Ofloxacin–Ticlopidine', 'Tolbutamide–Vincristine', 'Panobinostat–Rosiglitazone', 'Hydralazine–Reserpine' and 'Ranitidine–Teniposide', deserve to be confirmed by further experiments. Additionally, the drug 'Vincristine' appears in three predicted DDIs, two of which have been confirmed. More attention should be paid on 'Tolbutamide–Vincristine'.

Especially, in order to study the potential DDIs, which are related to a given disease, we generate the disease-related drugs from CTD database. Those drugs have been used to treat the given disease. In our datasets, the numbers of breast, colorectal and lung neoplasms-related drugs are 64, 31 and 36, respectively. The unknown DDIs that are connected with those drugs are predicted. The predicted results are listed in Tables 4, 5, and 6.

In the predicted results of breast neoplasms-related DDIs, 7 out of 10 DDIs have been confirmed to have interactions in either TWOSIDE or Drugs.com. Especially, there are two confirmed DDIs, each of which consists of two breast neoplasms-related drugs. The other three DDIs, 'Sulindac–Methazolamide', 'Sulindac–Theobromine' and 'Ranitidine–Teniposide', deserve to be confirmed by further experiments. Especially, among the 10 predicted DDIs, the drug 'Ranitidine' appears in four DDIs, whereas three DDIs have been confirmed. The DDI 'Ranitidine–Teniposide' should attract more attention.

Table 6. The top ten predicted DDIs of lung neoplasms-related drugs

Rank	Drug A	Drug B	Evidence Source	Description
1	**Sulindac**	Methazolamide	N.A.	N.A.
2	**Rosiglitazone**	Metformin	TWOSIDE	Using the drug combination may increase the side effect of anaemia vitamin b12 deficiency.
3	**Theophylline**	**Vincristine**	TWOSIDE	Using the drug combination may increase the side effect of neutropenia.
4	**Sulindac**	Theobromine	N.A.	N.A.
5	**Methotrexate**	Meloxicam	TWOSIDE	Using the drug combination may increase the side effect of iron deficiency anaemia.
6	**Theophylline**	Thalidomide	TWOSIDE	Using the drug combination may increase the side effect of anaemia.
7	**Ifosfamide**	Ofloxacin	Drugs.com	Chemotherapy with ifosfamide may reduce the plasma concentrations of oral ofloxacin.
8	**Theophylline**	Olanzapine	TWOSIDE	Using the drug combination may increase the side effect of anaemia.
9	**Sulindac**	Isosorbide	TWOSIDE	Using the drug combination may increase the side effect of pancytopenia.
10	**Melatonin**	Tacrolimus	TWOSIDE	Using the drug combination may increase the side effect of pancytopenia.

The lung neoplasms-related drugs are in bold.

In the predicted results of colorectal neoplasms-related DDIs, 7 out of 10 DDIs have been confirmed to have interactions in TWOSIDE. The other three interactions, 'Dacarbazine–Phenytoin', 'Fluorouracil–Oxymetholone' and 'Doxorubicin–Lynestrenol', could be potential DDIs.

In the predicted results of lung neoplasms-related DDIs, 8 out of 10 DDIs have been confirmed to have interactions in either TWOSIDE or Drugs.com. The other two DDIs, 'Sulindac–Methazolamide' and 'Sulindac–Theobromine', are also on the predicted list of breast neoplasms.

These neoplasms-related case studies demonstrate the usefulness of our GCNMK model in identifying potential DDIs for specific disease-related drugs.

Conclusion and Discussion

In this study, we have proposed a GCNMK model for predicting DDIs. The 'increase'-related DDIs and 'decrease'-related DDIs are used to construct two DDI graphs, which are the graph kernels in our model. Then novel embeddings of drugs are produced by three GCN blocks. A DDI feature vector is the concatenation of two drug feature vectors. A block of three fully connected layers is used as a predictor. Comprehensive experiments have been conducted to evaluate the performance of GCNMK and other methods. In the experiments, our GCNMK model outperforms all other methods. In the case studies, most of the predicted DDIs have evidence to support the existence of their interactions. Therefore, benefiting from the two graph kernels, our GCNMK model can be used to predict DDIs effectively.

Even so, there is a limitation in our proposed model. When constructing the DDI graphs and generating the set of drugs, the drugs in the experiment have at least one DDI. We remove the drugs that do not have any known DDIs. As a result, our model can not identify DDIs among isolated drugs.

There are several directions of future work along this study. In the DDI graphs of GCNMK, the edges belong to the same type. We could adapt this to any heterogeneous network, such as drug–disease network. The descriptions of drug–diseases associations consist of two types: therapeutic and marker/mechanism, which may be useful for employing a GCN model. Another future direction is to distinguish more types of predicted DDIs. According to their functions, each type of DDI may be used to construct a graph kernel, and the model has potential to identify the specific type of a predicted DDI.

Key Points

- We propose a graph convolutional network with multi-kernel, termed GCNMK, for predicting DDIs.
- The DDIs are divided into two groups, which are increased and decreased DDIs.
- GCNMK uses GCN blocks to capture structure features from both increased and decreased DDI graphs and uses fully connected layers as the predictor.

Data availability

The datasets were derived from the following sources in the public domain: the drug–drug interactions from https://www.drugbank.ca/, the drug–enzyme associations from https://www.drugbank.ca/ [23], the pathway–target associations from https://www.genome.jp/kegg/pathway.html [25] and http://ctdbase.org/ [24], the drug–side effect associations from http://sideeffects.embl.de/ [26], the drug chemical substructures from

https://www.drugbank.ca/, the drug–target associations from https://www.drugbank.ca/ and http://ctdbase.org/, the drug perturbation profiles from https://www.ncbi.nlm.nih.gov/geo/query/acc.cgi?acc=GSE92742 [28].

Acknowledgments

The authors thank the anonymous reviewers for their valuable suggestions.

Author contributions statement

F.W. and F.X.W. discussed the algorithms and conceived the experiments; F.W. implemented the algorithms and experiments, analyzed the results and wrote the manuscript; F.X.W., X.L. and B.L. reviewed the manuscript.

Funding

Natural Science and Engineering Research Council of Canada (NSERC); China Scholarship Council (CSC); the National Natural Science Foundation of China (Grant No. 2020YFB2104400, 61428209).

References

1. Pushpakom S, Iorio F, Eyers PA, *et al.* Drug repurposing: progress, challenges and recommendations. *Nat Rev Drug Discov* 2019;**18**(1):41–58.
2. Luo H, Wang J, Li M, *et al.* Drug repositioning based on comprehensive similarity measures and Bi-Random walk algorithm. *Bioinformatics* 2016;**32**(17):2664–71.
3. Luo H, Wang J, Li M, *et al.* Computational drug repositioning with random walk on a heterogeneous network. *IEEE/ACM Trans Comput Biol Bioinform* 2018;**16**(6):1890–900.
4. Jiang HJ, Huang YA, You ZH. Predicting drug-disease associations via using gaussian interaction profile and kernel-based autoencoder. *Biomed Res Int* 2019;**2019**:1–11.
5. Li Z, Huang Q, Chen X, *et al.* Identification of drug-disease associations using information of molecular structures and clinical symptoms via deep convolutional neural network. *Front Chem* 2020;**7**:1–14.
6. Yu Z, Huang F, Zhao X, *et al.* Predicting drug-disease associations through layer attention graph convolutional network. *Brief Bioinform* 2021;**22**(4):1–11.
7. Wang F, Ding Y, Lei X, *et al.* Identifying gene signatures for cancer drug repositioning based on sample clustering. *IEEE/ACM Trans Comput Biol Bioinform* 2020;1–13. 10.1109/TCBB.2020.3019781.
8. Luo Y, Zhao X, Zhou J, *et al.* A network integration approach for drug-target interaction prediction and computational drug repositioning from heterogeneous information. *Nat Commun* 2017;**8**(1):1–13.
9. Wen M, Zhang Z, Niu S, *et al.* Deep-learning-based drug-target interaction prediction. *J Proteome Res* 2017;**16**(4):1401–9.
10. Wang H, Wang J, Dong C, *et al.* A novel approach for drug-target interactions prediction based on multimodal deep autoencoder. *Front Pharmacol* 2020;**10**:1–19.
11. Hu S, Zhang C, Chen P, *et al.* Predicting drug-target interactions from drug structure and protein sequence using novel convolutional neural networks. *BMC Bioinformatics* 2019;**20**(25):1–12.
12. Monteiro NRC, Ribeiro B, Arrais J, *et al.* Drug-target interaction prediction: end-to-end deep learning approach. *IEEE/ACM Trans Comput Biol Bioinform* 2020;1–12. 10.1109/TCBB.2020.2977335.
13. Jiang M, Li Z, Zhang S, *et al.* Drug-target affinity prediction using graph neural network and contact maps. *RSC Adv* 2020;**10**(35):20701–12.
14. Ferdousi R, Safdari R, Omidi Y. Computational prediction of drug-drug interactions based on drugs functional similarities. *J Biomed Inform* 2017;**70**:54–64.
15. Yan C, Duan G, Pan Y, *et al.* DDIGIP: predicting drug-drug interactions based on Gaussian interaction profile kernels. *BMC Bioinformatics* 2019;**20**(15):1–10.
16. Zheng Y, Peng H, Zhang X, *et al.* DDI-PULearn: a positive-unlabeled learning method for large-scale prediction of drug-drug interactions. *BMC Bioinformatics* 2019;**20**(19):1–12.
17. Zhou B, Wang R, Wu P, *et al.* Drug repurposing based on drug-drug interaction. *Chem Biol Drug Des* 2015;**85**(2):137–44.
18. Zhang W, Chen Y, Liu F, *et al.* Predicting potential drug-drug interactions by integrating chemical, biological, phenotypic and network data. *BMC Bioinformatics* 2017;**18**(1):1–12.
19. Feng YH, Zhang SW, Shi JY. DPDDI: a deep predictor for drug-drug interactions. *BMC Bioinformatics* 2020;**21**(1):1–15.
20. Huang K, Xiao C, Glass LM, *et al.* SkipGNN: predicting molecular interactions with skip-graph networks. *Sci Rep* 2020;**10**(1):1–16.
21. Zhang Y, Qiu Y, Cui Y, *et al.* Predicting drug-drug interactions using multi-modal deep auto-encoders based network embedding and positive-unlabeled learning. *Methods* 2020;**179**:37–46.
22. Kipf TN, Welling M. Semi-supervised classification with graph convolutional networks. arXiv preprint arXiv:1609.02907. 2016;1–14.
23. Wishart DS, Feunang YD, Guo AC, *et al.* DrugBank 5.0: a major update to the DrugBank database for 2018. *Nucleic Acids Res* 2018;**46**(D1):D1074–82. 10.1093/nar/gkx1037 [dataset].
24. Davis AP, Grondin CJ, Johnson RJ, *et al.* Comparative toxicogenomics database (CTD): update 2021. *Nucleic Acids Res* 2021;**49**(D1):D1138–43. 10.1093/nar/gkaa891.
25. Kanehisa M, Furumichi M, Sato Y, *et al.* KEGG: integrating viruses and cellular organisms. *Nucleic Acids Res* 2021;**49**(D1):D545–51. 10.1093/nar/gkaa970.
26. Kuhn M, Letunic I, Jensen L, *et al.* The SIDER database of drugs and side effects. *Nucleic Acids Res* 2016;**44**(D1):D1075–9. 10.1093/nar/gkv1075.
27. Grover A, Leskovec J. node2vec: Scalable feature learning for networks. In: *Proceedings of the 22nd ACM SIGKDD international conference on knowledge discovery and data mining*. Association for Computing Machinery, New York, NY, USA, 2016, 855–64.
28. Subramanian A, Narayan R, Corsello SM, *et al.* A next generation connectivity map: L1000 platform and the first 1,000,000 profiles. *Cell* 2017;**171**(6):1437–52. 10.1016/j.cell.2017.10.049.
29. Iorio F, Bosotti R, Scacheri E, *et al.* Discovery of drug mode of action and drug repositioning from transcriptional responses. *Proc Natl Acad Sci* 2010;**107**(33):14621–6.
30. Tatonetti NP, Patrick PY, Daneshjou R, *et al.* Data-driven prediction of drug effects and interactions. *Sci Transl Med* 2012;**4**(125):1–26.
31. Drugs.com. Drug Interactions Checker. https://www.drugs.com/drug_interactions.html, September 13, 2021.
32. Laurens VM, Geoffrey H. Visualizing data using t-SNE. *J Mach Learn Res* 2008;**9**(11):1–27.